

Strain, anisotropy of anhysteretic remanence, and anisotropy of magnetic susceptibility in a slaty tuff

Norihiro Nakamura^{a,*}, Graham J. Borradaile^b

^a *The Tohoku University Museum, Tohoku University, Sendai 980-8578, Japan*

^b *Geology Department, Lakehead University, Thunder Bay, Ont., Canada P7B 5E1*

Received 22 November 2000; received in revised form 14 May 2001; accepted 24 May 2001

Abstract

Finite strain data for the Borrowdale slaty tuffs compare variably with the anisotropy of magnetic susceptibility (AMS) and anisotropy of anhysteretic remanent magnetization (AARM). Finite strain, determined from lapilli-rims, shows that slaty cleavage was formed by coaxial flattening with $X:Y:Z$ in the ratio 1.74:1.21 and 0.48. AARM was measured in different coercivity windows to isolate contributions from magnetite of different grain sizes: (a) 0–3 mT for multi-domain (MD), (b) 3–15 mT for pseudo-single-domain (PSD) and (c) 15–60 mT for single-domain (SD). AMS combines petrofabric contributions from silicates as well as magnetite. Magnetite grains may grow, recrystallize or rearrange domains after or during metamorphism and postdate or overlap with the silicate's fabric evolution. AMS foliation, defined by paramagnetic chlorites, is parallel to slaty cleavage. AARM foliation for SD magnetites is offset clockwise from AMS foliation, which may reflect late crystallization or domain-rearrangement of magnetites in response to a latter noncoaxial increment. AMS fabric-shape consistently corresponds to strain ellipsoids and indicates that the strain-induced AMS fabric is susceptible to the change of oblateness rather than strain intensity. Furthermore, investigation of the different AARM subfabrics and finite strain shows that only SD magnetite's AARM correlates with finite strain, and weakly at that. © 2001 Elsevier Science B.V. All rights reserved.

Keywords: Anisotropy of anhysteretic remanence; Coercive force; Anisotropy of magnetic susceptibility; Slate

1. Introduction

We compare finite strain, anisotropy of magnetic susceptibility (AMS) and anisotropy of anhysteretic remanent magnetization (AARM) from the same samples of a slaty tuff. AMS summarizes all magnetic contributions (i.e. diamagnetic, paramagnetic and ferromagnetic minerals) whereas AARM reflects the

anisotropy component due to orientation distribution of remanence-bearing or ferromagnetic minerals (McCabe et al., 1985; Jackson, 1991). The first attempt to isolate a fabric of ferromagnetic minerals from the matrix was Henry and Daly (1983), using anisotropy of saturation isothermal remanent magnetization (ASIRM). Although usually successful, ASIRM risks nonlinear susceptibility effects where strong magnetic field is required to achieve measurable remanences (Daly and Zinsser, 1973; Borradaile and Dehls, 1993). AARM has been used previously to infer the tectonic deformation history on a slaty cleavage (Housen and van der Pluijm, 1991), of a weakly deformed Archean anorthosite (Borradaile et al., 1998), and in granite using two different coercive force windows (Trindade

* Corresponding author. Present address: Geology Department, Lakehead University, Thunder Bay, Ont., Canada P7B 5E1. Fax: +1-807-346-7853.

E-mail addresses: norihiro.nakamura@lakeheadu.ca, n-naka@mail.cc.tohoku.ac.jp (N. Nakamura), borradaile@lakeheadu.ca (G.J. Borradaile).

et al., 1999). However, there are few comparisons of AARM with finite strain, and still fewer with multiple coercive force windows.

Studies of the Borrowdale volcanic sequence, in the Ordovician slaty rocks of the English Lake district have described its petrology, structure, strain and magnetic properties (Oertel, 1970; Moseley, 1972; Bell, 1981; Borradaile et al., 1985; Henry, 1990). The slaty rocks experienced a single fabric-forming tectonic episode during greenschist facies regional metamorphism of the Caledonian tectonic deformation phase (Moseley, 1972; Borradaile et al., 1985). Rathore (1980) showed the dominant ferromagnetic mineral is magnetite from Curie point determination. Also, isothermal remanence acquisition and SEM petrography revealed that submicron magnetite (not hematite) may be hosted in the paramagnetic chlorite (Borradaile et al., 1985). Borradaile et al. (1985) determined from X-ray diffraction that the AMS is carried by a matrix-forming paramagnetic chlorite of diabantite–ripidolite composition, which has recrystallized during the deformation. Previous magnetic fabric studies were limited to observations of the anisotropy of low field susceptibility (AMS), (e.g. Rathore, 1980; Kligfield et al., 1981; Borradaile and Mothersill, 1984). We extend that work by comparing AMS with AARM with different coercive force

windows. Unlike some other authors, we used the *same* samples for AMS, AARM and strain measurements because intra-sample heterogeneity exceeds regional variation in the Borrowdale volcanic rocks (Borradaile and Mothersill, 1984). The comparison of magnetic subfabrics with strain is simplified by a single, penetrative coaxial strain history.

Acquisition of anhysteretic remanent magnetization (ARM) is hindered by coercivity of remanence (Jackson, 1991). Coercivity of remanence (H_{cr}) is related to and exceeds the coercive force H_c . For magnetite (magnetically soft mineral), the coercive force can be related to grain-size (d) by a power-law function as

$$H_c \sim d^{-n} \quad (1)$$

where n varies from 0 to 1 (Day et al., 1977; Dunlop and Özdemir, 1997). Grains in the size range d_2 – d_1 , where $d_2 > d_1$ acquire ARM when exposed to a weak direct current field (dc) superimposed over an alternating field (AF) window ($H_{c1} \sim H_{c2}$), while the rest of the assemblage is demagnetized from a peak field $>H_{c1}$ (Fig. 1). H_{c1} is the uppermost coercive force limit associated with grain-size d_1 . Jackson et al. (1988) first showed the principle of isolating different orientation of distributions of different magnetite subfabrics by using different coercive force

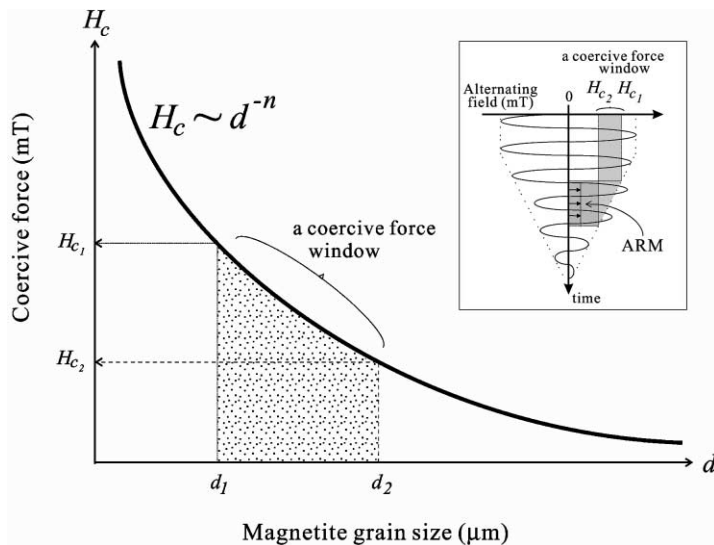


Fig. 1. Acquisition of an ARM of magnetite grain in a size range by changing a coercive force window, using an empirical power law equation of $H_c \sim d^{-n}$.

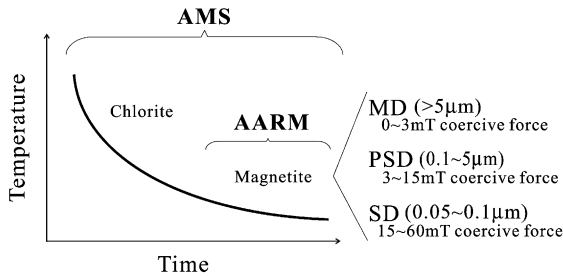


Fig. 2. Schematic diagram of recrystallization of metamorphic minerals. AMS summarizes the contribution of all minerals and AARM isolates the fabrics of later growth magnetite: MD, PSD and SD one.

windows for the same sample. They called this partial anisotropy of anhysteretic remanent magnetization (pAARM). In greenschist facies metabasic volcanic rocks, chlorite-growing reactions produce fine-grained magnetite inclusions at the expense of the original igneous mafic silicates (Suk et al., 1990; Housen et al., 1993a; Borradaile, 1994). The magnetite inclusions may grow, recrystallize or change their domain structure after phyllosilicate growth during metamorphism (Fig. 2). In metamorphic rocks, later magnetite growth may produce smaller grains and, thus higher coercive grains may preserve a later glimpse of the strain-field dynamics. We divided the AF decay range into three window based on results of pilot tests: (a) 0–3 mT for the multi-domain (MD) size magnetite; (b) 3–15 mT for the pseudo-single-domain (PSD) and (c) 15–60 mT for the single-domain (SD). Over 60 mT, no volume of magnetite was activated for the acquisition of ARM. Those coercive force windows should isolate the partial orientation distribution of MD, PSD and SD magnetites, although there is no adequate theory of a remanence behavior for PSD grains (Merrill, 1970; Levi and Merrill, 1978; Dunlop and Özdemir, 1997). The pAARM ellipsoid for each coercive force window was determined from the body-diagonal seven-orientation scheme of Borradaile and Stupavsky (1995).

Several workers have addressed the correlation of the AMS ellipsoid (tensor) with that of finite strain (Rathore, 1979, 1980; Kligfield et al., 1981; Borradaile and Mothersill, 1984; Cogné and Perroud, 1988; Hirt et al., 1988; Borradaile, 1991; Borradaile and Henry, 1997). Valid correlations generally require maximum shortening >30%, so that primary AMS

fabrics are sufficiently overprinted. The shortening should be <70%, otherwise mineral alignments are saturated and anisotropy degree achieves a plateau, although plastic deformation of magnetite could produce more anisotropic AMS fabric in high-strain ultramylonites under granulite metamorphic facies (Housen et al., 1995). The orientations of principal magnetic susceptibilities correlate well with principal strain orientations, whereas there is no correlation between strain magnitudes and principal susceptibility magnitudes on the Flinn diagram (Borradaile and Mothersill, 1984). Although that diagram is familiar to structural geologists, it has the disadvantage that the axes represent neither shape of symmetry nor ellipsoidal intensity of AMS fabric uniquely. On the other hand, the Jelinek diagram permits statistical comparison of fabric-shapes by using parameters of a symmetrical shape description: T_j (oblate to prolate; +1 to -1) in contrast to Flinn's k -value (0–∞) and an ellipsoidal intensity P_j (sphere to ellipsoid; 1–∞) which includes reference to the intermediate value (Jelinek, 1981). Housen and van der Pluijm (1991) showed close correspondence of AARM fabric with strain induced rock fabrics due to cleavage formation, in the coercive force window 0–30 mT in a shale-to-slate transition. However, the correlation between AARM and finite strain was unclear in the absence of finite strain markers.

2. Strain and anisotropy of magnetic susceptibility (AMS)

We used the selvage strain method for the concentrically rimmed accretionary lapilli. Previous strain studies merely used the shapes of lapilli to estimate strain (Rathore, 1979, 1980), involving poorly justified assumptions concerning about the original fabric, and initial shapes of lapilli. However, our strain analysis technique avoids unknown initial shape and preferred orientation, because the multiple concentric layering of many lapilli allows each individual lapillus to act as a strain marker (Borradaile and Mothersill, 1984; Borradaile, 1987). The mean strain ratio $X:Y:Z$ is 1.74:1.21:0.48.

AMS is primarily dominated by the effects of strongly oriented phyllosilicates (Borradaile et al., 1985), in this study paramagnetic chlorites. Fig. 3

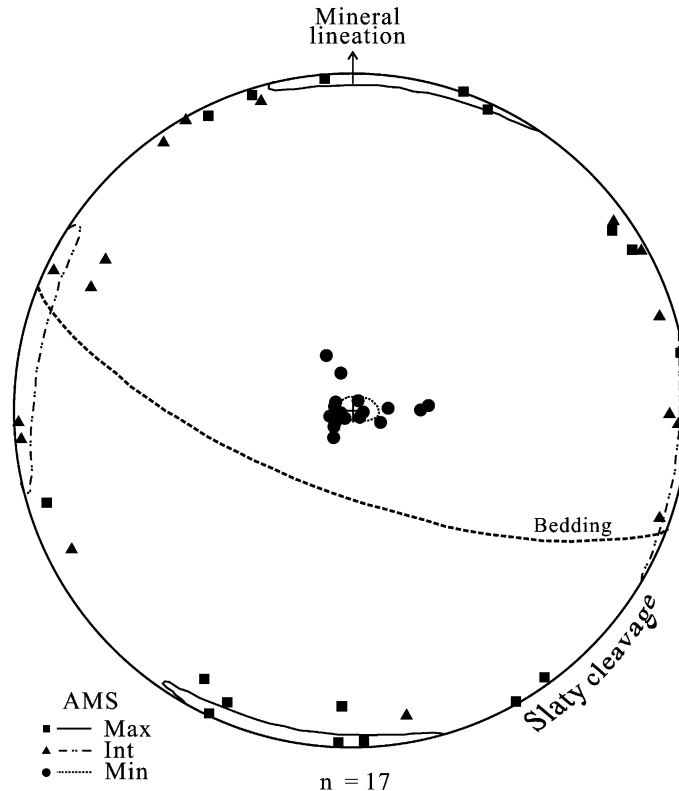


Fig. 3. Principal directions of the anisotropy of susceptibility of low field, induced magnetization (AMS) with unweighted 95% confidence zones about tensor-mean directions (Jelinek, 1978). The minimum principal axes are perpendicular to slaty cleavage. The maximum axes are subparallel to the mineral lineation and elongation of lapilli. The dotted line represents the bedding plane.

shows the lower hemisphere stereogram projection of AMS principal directions, from which we can identify a magnetic foliation and lineation with unweighted 95% confidence zones about the tensor-mean axes (Jelinek, 1978). The 95% confidence ellipses around the mean maximum, intermediate and minimum principal directions are small and define an orthorhombic orientation distribution with a strong oblate component. The AMS fabric reveals no bedding-parallel fabric. Magnetic foliation is entirely parallel to slaty cleavage with partial girdles of maximum principal axes (k_{\max} plotted as squares) and intermediate axes (k_{int}), and magnetic lineation (k_{\max}) parallels the long-axes of deformed lapilli. Minimum susceptibility axes (k_{\min}) are perpendicular to slaty cleavage.

The Jelinek diagram permits comparison of fabric shape with strain (Fig. 4a). T_j reveals the symmetry of the ellipsoid, with +1 for oblate ellipsoids ($k_{\text{int}} =$

k_{\max}), 0 for orthorhombic and –1 for prolate ellipsoids ($k_{\text{int}} = k_{\min}$). The intensity of the fabric or eccentricity is represented by P_j with $P_j = 1$ for a sphere or isotropic fabric. Thus, the Jelinek diagram represents the relationship between the shape of symmetry and the ellipsoid intensity of fabric anisotropy.

The phyllosilicate matrix fabric (AMS) records stronger flattening ($T_j = 0.6\text{--}0.9$) than the strain fabric ($T_j = 0.1\text{--}0.7$) because a coaxial stress field produced a more perfect, near-saturation alignment of chlorite during syntectonic recrystallization. Consistent tie lines slopes indicate a good correlation between strain and AMS fabrics (each tie line joins strain and AMS ellipsoid data from the same sample). The slopes are well constrained between –0.004 and –0.263 (mean: -0.131 ± 0.073) and rarely intersect. The one-to-one correspondence of the tie lines indicates statistically that the higher T_j value of strain

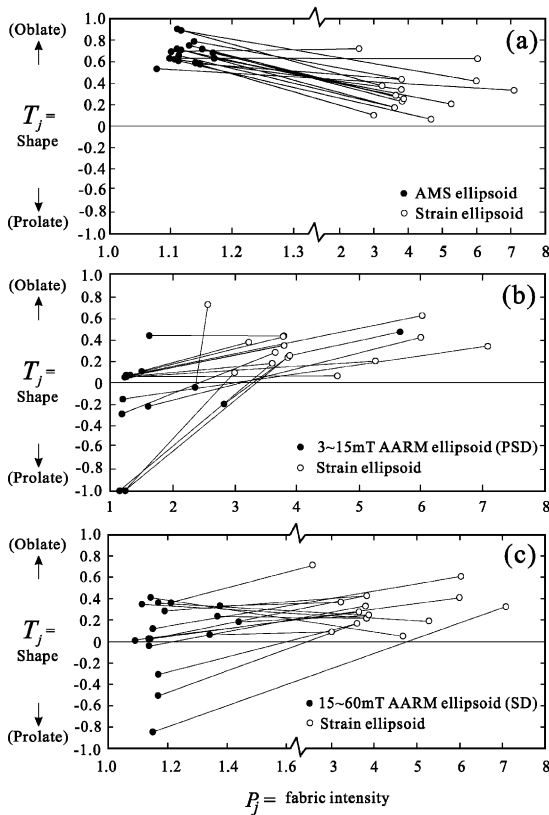


Fig. 4. Fabric plot of Borrowdale volcanic tuffs with accretionary lapilli using the parameters of Jelinek (1981). (a) AMS, (b) AARM of PSD magnetites with 3–15 mT coercive force window and (c) AARM of SD ones with 15–60 mT coercive force window. Some samples share same strain coordinates.

corresponds to the higher T_j for AMS. The negative dependence of AMS on strain means that the oblateness of the AMS ellipse is greater than that of strain. We believe that this new representation of the correlation between strain and AMS ellipsoids, although simple, more effectively compares the respective tensors. The parallelism of the tie lines implies a genetic influence of strain on the paramagnetic silicates that dominate the AMS fabric.

3. Anisotropy of anhysteretic remanent magnetization (AARM) and strain

Anisotropy of anhysteretic remanent magnetization (AARM), e.g. McCabe et al. (1985) and Jackson

(1991), was determined with a SI-4 (Sapphire Instruments), nontumbling static AF demagnetizer and a Molspin magnetometer. Our ARM was acquired by subjecting samples to a small direct current field of 0.1 mT during AF demagnetization down from 100 to 0 mT. The body-diagonal scheme ensures that each AF demagnetization and ARM application was non-orthogonal to the previous step in the determination of ARM anisotropy. This scheme minimizes the risk of gyroremanent magnetization acquisition (Stephenson, 1980, 1993), which however our spinner magnetometer program can detect.

Dunlop and Özdemir (1997) compiled coercive force data for different grain sizes of hydrothermally grown (low defect density) and crushed magnetites (induced defects). They found the coercive force varies as d^{-n} with $n = 0.4–0.6$ in magnetite above critical SD size. A size dependence of H_c proportional to $d^{-1/2}$ can be attributed to domain walls pinned by ordered arrays of defects, such as dislocations (Stacey and Wise, 1967). In this study, we regarded the magnetite grain sizes of over $5 \mu\text{m}$ as MD; $5–0.1 \mu\text{m}$ as PSD and $0.05–0.1 \mu\text{m}$ as SD. These grain sizes correspond broadly to three coercive force windows of 0–3 mT for MD, of 3–15 mT for PSD and of 15–60 mT for SD magnetite according to Eq. (1).

Stereograms show scattered principal AARM directions, in comparison with AMS (cf. Figs. 5 and 3). The coercive force window of 0–3 mT has no definable mean tensor because MD magnetite orientations distribute randomly (Fig. 5a). Only a feeble preferred orientation distribution of AARM is recognized for PSD magnetite (Fig. 5b) with very wide 95% confidential circle limit about the tensor-mean directions of k_{max} , k_{int} and k_{min} , that are unacceptable (Jelinek, 1978; Lienert, 1991). Only SD magnetite shows a clear preferred orientation with an orthorhombic symmetry (Fig. 5c). The principal axes for the pAARM of SD magnetite differ from those of AMS (cf. Figs. 3 and 5c), with AARM axes rotated clockwise from those of AMS. Larger, MD and PSD magnetite is so feebly oriented that it contributes negligibly to the AMS fabric (cf. Figs. 3, 5a and b).

MD magnetite yields no meaningful fabric correlation with finite strain. However, PSD magnetite reveals some consistent strain-AARM fabric correlations (Fig. 4b). These tentatively indicate that the PSD magnetite fabric is independent of the older silicate

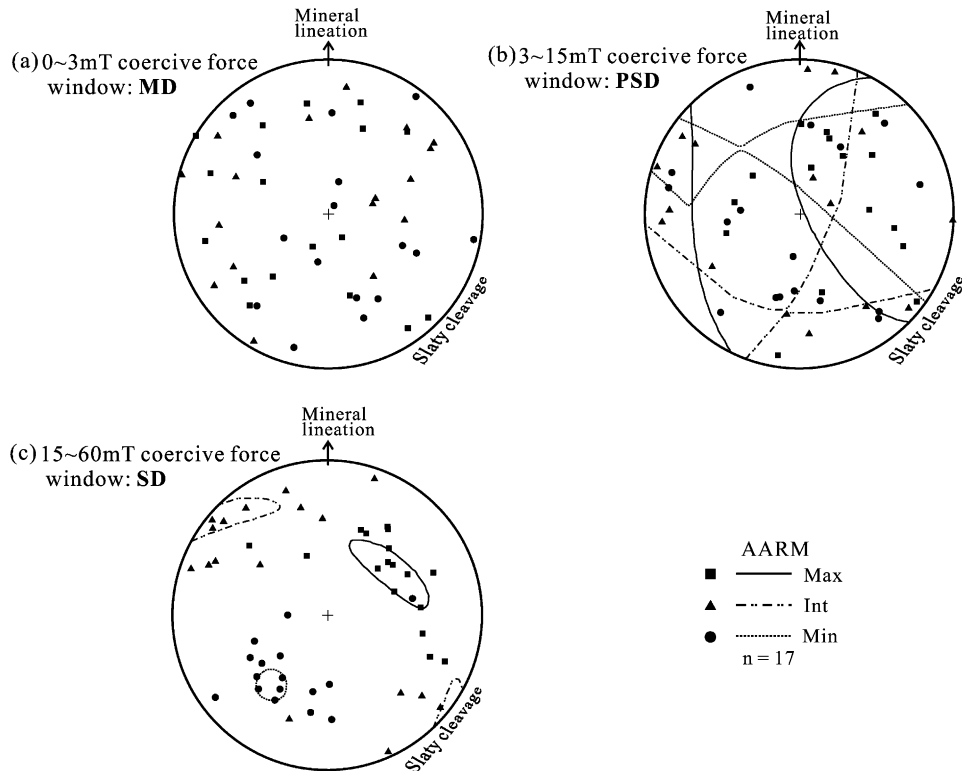


Fig. 5. Principal directions of AARM. Only SD magnetite shows a well-defined orientation distribution.

fabric elements due to coaxial flattening. In contrast, SD magnetite shows a very well-defined orthorhombic fabric compatible with tectonic flattening ($0 < T_j < +1$) despite magnetite grains usually possessing an intrinsic prolate grain-AARM (Fig. 4c). Although the slopes of tie lines occasionally intersect for SD magnetites, the slopes of the AARM-strain tie lines vary from -0.1 to 0.279 (mean: 0.090 ± 0.110) and correlate positively with strain. Exceptional negative slopes may be due to heterogeneity of strain or mineralogy.

4. Discussions and conclusions

In these rocks, Rathore (1980) attempted to correlate AMS and strain by plotting logarithmic, normalized values of k_{\max} , k_{int} and k_{\min} , against normalized principal strain values derived from the simple lapilli shapes. However, the correlation erroneously linked dependent values (Borradaile and Mothersill, 1984).

Thus, the global power-law correlation for AMS and strain may give misleading correlations occasionally (Rathore, 1979, 1980; Kligfield et al., 1981). Here, we recommend tensor correlation by Jelinek's parameters to provide a simple but effective comparison of the respective AMS, AARM and strain tensors. This diagram has the advantage of representing the tensor properties as a symmetry element and an ellipsoid intensity, and parallel tie-lines corroborate the view that strain induced the change in magnetic symmetry. Using the Jelinek diagram, we found that the strain-induced alignment of silicates is susceptible to the change of oblateness (symmetry element) of the AMS fabric rather than its intensity.

For our rocks, the finer magnetite fabrics (i.e. SD with 15–60 mT) correspond weakly with finite strain, whereas MD and PSD magnetite fails to show such consistent relations (Fig. 4). The phyllosilicate matrix fabric (AMS) records the strong flattening due to the saturated preferred dimensional alignment of

chlorites during syntectonic recrystallization and its fabric clearly correlated with finite strain fabric due to a coaxial stress field. Conversely, the AARM shapes are quite scattered for PSD and MD magnetite, and independent of strain. For SD magnetite, however, the clear orthorhombic shape fabric reflects the effect of oblate flattening in a coaxial stress field in spite of the intrinsic prolate AARM of magnetite. This result indicates that AARM shape fabrics can be weakly affected by the later stress field.

In many metamorphic rocks, inclusions or exsolved micrograins of magnetite are recrystallized during deformation-induced metamorphic process. They do not have an independent orientation distribution and their preferred orientation is dictated locally by the crystal symmetry of the host minerals (Borradaile, 1994). This means that a magnetite inclusion fabric may be coaxial to a host mineral fabric. Housen and

van der Pluijm (1991) studied the transition from undeformed shale to slate in the Martinsburg formation, and found that pAARM for a 0–30 mT coercive force window detected a fabric that progressively changed from bedding-normal to cleavage-normal, with inferred increasing strain. Their coercive force window for AARM corresponds to MD and PSD magnetite. Their result shows that the host mineral fabric is parallel to the AARM magnetite one. Our result clearly shows that AARM magnetite fabric differs from phyllosilicate matrix fabric (AMS) (Fig. 6), although the AARM foliation is nearly perpendicular to bedding. Preferential alignment of dislocations can give rise to anisotropy in MD/PSD grains with a minor shape effect, whereas shape effects are probably the dominant factor in the SD grains (R.T. Merrill, Personal comm.). Therefore, the AARM in the SD grains is controlled by the shape of recrystallized magnetites

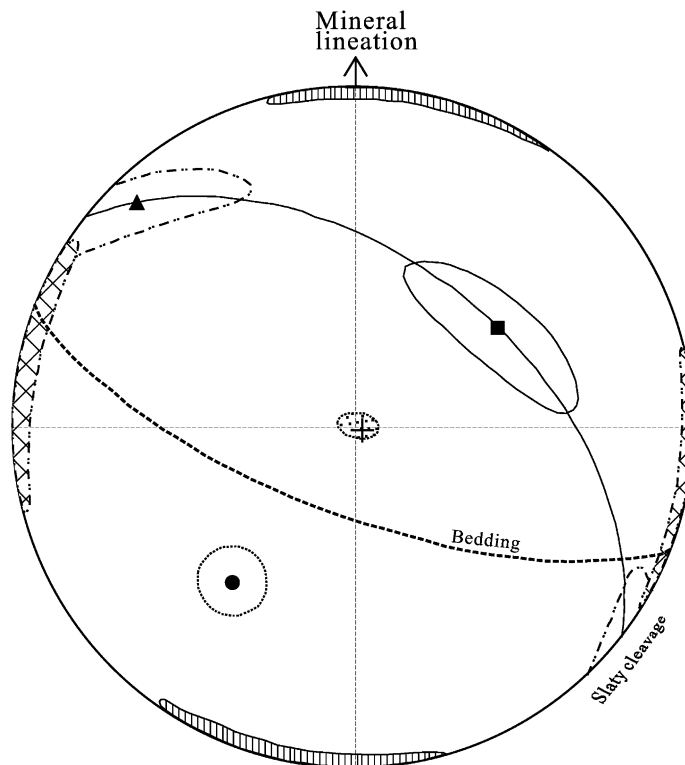


Fig. 6. Superimposed stereogram of AMS for silicate fabric and AARM for SD magnetite fabric. The discrepancy shows a clockwise offset in response to latter phases of a noncoaxial stress history. Solid girdle is a magnetic foliation of AARM maximum principal axes and intermediate axes at a high angle to bedding.

that grew during metamorphism in a later stress field. Thus, the recrystallized magnetites are likely to produce a noncoaxial fabric to host crystal symmetry.

We have discriminated cryptic deformation fabrics by the utility of magnetic fabric techniques consisting of AMS, and partial AARM that is grain-size dependent. Because the ARM is feeble indicating the paucity of remanence-carrying grains, they contribute little to AMS. The AMS inverse fabric from SD magnetite is still weaker than of “normal” PSD and MD magnetite so that its contribution can be neglected. There are also no composite magnetic fabrics from SD magnetite and chlorite (Fig. 6), which could produce an AMS maximum direction parallel to the intersection of the AMS magnetic foliation and the pAARM foliation planes (Housen et al., 1993b). Therefore, the AMS is controlled by paramagnetic chlorites and mainly records the older strain dynamics due to a coaxial oblate stress field that produced the schistose fabric during chlorite crystallization. AARM records later glimpses of the strain-field dynamics from younger magnetite grains. Thus, we can infer the change in regional kinematics from the comparison of the AMS and AARM fabric orientations (Borradaile et al., 1993; Werner and Borradaile, 1996; Borradaile et al., 1998; Trindade et al., 1999). The AARM principal axes systematically rotate clockwise from those of AMS (Fig. 6). This clear discrepancy may indicate the late crystallization or domain-rearrangement of magnetites during a differently oriented stress-field, implying that this part of the Borrowdale volcanic sequence may have experienced large, syn-metamorphic transpression, i.e. simultaneous compression and shear.

Acknowledgements

We thank R.T. Merrill and B. Housen for their valuable comments. This work was funded by NSERC operating and equipment grants to Graham Borradaile. Norihiro Nakamura was supported by the JSPS post-doctoral fellowships for research abroad during his stay in Canada.

References

- Bell, A.M., 1981. Strain factorisations from lapilli tuff, English Lake District. *J. Geol. Soc. London* 138, 463–474.
- Borradaile, G., Mothersill, J.S., 1984. Coaxial deformed and magnetic fabrics without simply correlated magnitudes of principal values. *Phys. Earth Planet. Int.* 35, 294–300.
- Borradaile, G., Mothersill, J., Tarling, D., Alford, C., 1985. Sources of magnetic susceptibility in a slate. *Earth Planet. Sci. Lett.* 76, 336–340.
- Borradaile, G., 1987. Analysis of strained sedimentary fabrics: review and tests. *Can. J. Earth Sci.* 24, 442–455.
- Borradaile, G., 1991. Correlation of strain with anisotropy of magnetic susceptibility (AMS). *Pure Appl. Geophys.* 135, 15–29.
- Borradaile, G., Dehls, J.F., 1993. Regional kinematic inferred from magnetic subfabrics in Archean rocks of Northern Ontario. *Canada J. Struct. Geol.* 15, 887–894.
- Borradaile, G., Werner, T., Dehl, J.F., Spark, R.N., 1993. Archean regional transpression and paleomagnetism in Northwestern Ontario. *Canada Tectonophysics* 220, 117–125.
- Borradaile, G., 1994. Paleomagnetism carried by crystal inclusions: the effect of preferred crystallographic orientation. *Earth Planet. Sci. Lett.* 126, 171–182.
- Borradaile, G., Stupavsky, M., 1995. Anisotropy of magnetic susceptibility: measurement schemes. *Geophys. Res. Lett.* 22, 1957–1960.
- Borradaile, G., Henry, B., 1997. Tectonic applications of magnetic susceptibility and its anisotropy. *Earth Sci. Rev.* 42, 49–93.
- Borradaile, G., Lagroix, F., King, D., 1998. Tilting and transpression of an Archean anorthosite in northern Ontario. *Tectonophysics* 293, 239–254.
- Cogné, J.P., Perroud, H., 1988. Anisotropy of magnetic susceptibility as a strain gauge in the Flamanville granite. NW France. *Phys. Earth Planet. Int.* 51, 264–270.
- Daly, L., Zinsser, H., 1973. Étude comparative des anisotropies de susceptibilité et d’aimantation rémanente isotherme: Conséquences pour l’analyse structurale et le paléomagnétisme. *Ann. Géophys.* 29, 189–200.
- Day, R., Fuller, M., Schmidt, V.A., 1977. Hysteresis properties of titanomagnetites: grain-size and compositional dependence. *Phys. Earth Planet. Int.* 13, 260–267.
- Dunlop, D., Özdemir, Ö., 1997. *Rock Magnetism: Fundamental and Frontiers*. Cambridge University Press, Cambridge.
- Henry, B., Daly, L., 1983. From qualitative to quantitative magnetic anisotropy analysis: the prospect of finite strain calibration. *Tectonophysics* 98, 327–336.
- Henry, B., 1990. Magnetic fabric implications for the relationships between deformation mode and grain growth in slates from the Borrowdale Volcanic Group in the English Lake District. *Tectonophysics* 178, 225–230.
- Hirt, A.M., Lowrie, W., Clendenen, W.S., Kligfield, R., 1988. The correlation of magnetic susceptibility with strain in the Chelmsford Formation of the Sudbury Basin. *Ont. Tectonophysics* 145, 177–189.
- Housen, B.A., van der Pluijm, B.A., 1991. Slaty cleavage development and magnetic anisotropy fabrics. *J. Geophys. Res.* 96, 9937–9946.
- Housen, B.A., van der Pluijm, B.A., Van der Voo, R., 1993a. Magnetite dissolution and neocrystallization during cleavage formation: paleomagnetic study of the Martinsburg Formation, Lehigh gap, Pennsylvania. *J. Geophys. Res.* 98, 13799–13813.

- Housen, B.A., Richter, C., van der Pluijm, B.A., 1993b. Composite magnetic anisotropy fabrics: experiments, numerical models, and implications for the quantification of rock fabrics. *Tectonophysics* 220, 1–12.
- Housen, B.A., van der Pluijm, B.A., Essene, E.J., 1995. Plastic behavior of magnetite and high strains obtained from magnetic fabrics in the Parry Sound shear zone, Ontario Grenville Province. *J. Struct. Geol.* 17, 265–278.
- Jackson, M., Gruber, W., Marvin, J., Banerjee, S.K., 1988. Partial anhysteretic remanence and its anisotropy: applications and grain-size-dependence. *Geophys. Res. Lett.* 15, 440–443.
- Jackson, M., 1991. Anisotropy of magnetic remanence: a brief review of mineralogical sources, physical origins, and geological applications, and comparison with susceptibility anisotropy. *Pure Appl. Geophys.* 136, 1–28.
- Jelinek, V., 1978. Statistical processing of magnetic susceptibility measured in groups of specimens. *Stud. Geophys. Geode.* 22, 50–62.
- Jelinek, V., 1981. Characterization of the magnetic fabric of rocks. *Tectonophysics* 79, T63–T67.
- Kligfield, R., Owens, W.H., Lowrie, W., 1981. Magnetic susceptibility anisotropy, strain, and progressive deformation in Permian sediments from the Maritime Alps (France). *Earth Planet. Sci. Lett.* 55, 181–189.
- Levi, S., Merrill, R.T., 1978. Properties of single domain, pseudo-single domain, and multidomain magnetite. *J. Geophys. Res.* 83, 309–323.
- Lienert, B.R., 1991. Monte Carlo simulation of errors in the anisotropy of magnetic susceptibility: a second-rank symmetric tensor. *J. Geophys. Res.* 96, 19539–19544.
- McCabe, C.M., Jackson, M., Ellwood, B.B., 1985. Magnetic anisotropy in the Trenton limestone: results of a new technique, anisotropy of anhysteretic susceptibility. *Geophys. Res. Lett.* 12, 333–336.
- Merrill, R.T., 1970. Low-temperature treatments of magnetite and magnetite-bearing rocks. *J. Geophys. Res.* 75, 3343–3349.
- Moseley, F., 1972. A tectonic history of northwest England. *J. Geol. Soc. London* 128, 561–598.
- Oertel, G., 1970. Deformation of a slaty, lapillar tuff in the Lake District. *England Geol. Soc. Am. Bull.* 81, 1172–1187.
- Rathore, J.S., 1979. Magnetic susceptibility anisotropy in the Cambrian slate belt of North Wales and correlation with strain. *Tectonophysics* 53, 83–97.
- Rathore, J.S., 1980. The magnetic fabrics of some slates from the Borrowdale volcanic group in the English Lake District and their correlations with strains. *Tectonophysics* 67, 207–220.
- Stacey, F.D., Wise, K.N., 1967. Crystal dislocations and coercivity in fine-grained magnetite. *Aust. J. Phys.* 20, 507–513.
- Stephenson, A., 1980. A gyromagnetic magnetization in anisotropic magnetic material. *Nature* 284, 49–51.
- Stephenson, A., 1993. Three-axis static alternating field demagnetization of rocks and the identification of natural remanent magnetization, gyromagnetic magnetization, and anisotropy. *J. Geophys. Res.* 98, 373–381.
- Suk, D., Peacor, D.R., Van der Voo, R., 1990. Replacement of pyrite framboids by magnetite in limestone and implications for paleomagnetism. *Nature* 345, 611–613.
- Trindade, R.I.F., Raposo, M.I.B., Ernesto, M., Siqueira, R., 1999. Magnetic susceptibility and partial anhysteretic remanence anisotropies in the magnetite-bearing granite pluton of Tourão, NE Braz. *Tectonophysics* 314, 443–468.
- Werner, T., Borradaile, G., 1996. Paleoremanence dispersal across a transpressed Archean terrain: deflection by anisotropy or by late compression? *J. Geophys. Res.* 101, 5531–5545.